Allergologia et immunopathologia
Sociedad Española de Inmunología Clínica, Alergología y Asma Pediátrica
www.all-imm.com

ORIGINAL ARTICLE

OPEN ACCESS

Knockdown of SHP2 attenuated LPS-induced ferroptosis via downregulating ACSL4 expression in acute lung injury

Bin Li[a], Zhan Wang[b], Jiayang Yuan[a], Dachuan Liang[a], Yanrong Cheng[c], Zheng Wang[c]*

[a]*Department of Infectious Diseases, Linfen People's Hospital, Linfen, Shanxi, China*
[b]*Research Division, National Health Commission of the People's Government of Linfen City, Linfen, Shanxi, China*
[c]*Intensive Care Unit, Linfen People's Hospital, Linfen, Shanxi, China*

Received 28 February 2023; Accepted 21 March 2023
Available online 1 May 2023

KEYWORDS
Acute Lung Injury;
SHP2;
Ferroptosis;
ACSL4

Abstract
Background: Acute lung injury (ALI) is a complex disease with a high mortality. Src homology 2 (SH2)-containing protein tyrosine phosphatase 2 (SHP2) is a protein tyrosine phosphatase that participates in pathogenesis of multiple diseases. Nevertheless, the role of SHP2 in ALI remains unknown.
Methods: The *in vivo* and *in vitro* lipopolysaccharide (LPS)-induced ALI models were successfully established. The histopathological changes were evaluated by hematoxylin and eosin staining. The vascular permeability of lungs was assessed by Evans blue assay. The expression of ACSL4 and SHP2 was detected by western blot and qRT-PCR assay. The lactate dehydrogenase (LDH) activity, malondialdehyde (MDA), iron, and glutathione (GSH) levels were measured by commercial kits.
Results: The SHP2 was upregulated in LPS-induced ALI mice and LPS-stimulated MLE-12 cells. In loss-of function experiment, the knockdown of SHP2 attenuated LPS-induced lung injury, microvessels damage, pulmonary edema, and increase of lung vascular permeability *in vivo*. Mechanically, shSHP2-rescued LPS induced increase in LDH activity, MDA, and iron levels, and decrease in GSH levels, as well as the accumulation of reactive oxygen species *in vivo* and *in vitro*, leading to an alleviation of LPS-induced ferroptosis. Notably, shSHP2 reduced the expression of Acyl-CoA synthetase long-chain 4 (ACSL4). In the rescued experiments, overexpression of ACSL4 abolished the shSHP2-induced reduction of LDH activity, MDA, and iron levels, and increase in GSH levels, thereby aggravating the LPS-induced ferroptosis.
Conclusion: These findings concluded that the knockdown of SHP2 attenuated LPS-induced ferroptosis via downregulation of ACSL4 expression in ALI, providing a novel sight for ALI treatment.

***Corresponding author:** Zheng Wang, Intensive Care Unit, Linfen People's Hospital, No. 319, Gulou West Avenue, Yaodu District, Linfen, Shanxi, China. *Email address*: wz_wangzheng0228@163.com.

https://doi.org/10.15586/aei.v51i3.856

Introduction

Acute lung injury (ALI) was first described in 1967, characterized by enhanced inflammation, dysfunction of alveolar–capillary membrane, and reduction in alveolar fluid clearance, eventually resulting in impaired gas exchange and pulmonary edema.[1-3] The pathogenesis of ALI is very complex, mainly involving the inflammatory reaction, apoptosis, autophagy, and pyrosis.[4] Although some progress has been made in the clinical diagnosis of ALI, there are still no specific treatments.[5] To data, the best therapeutic strategy against ALI is protective ventilation, but the mortality of ALI remains unchanged at approximately 40%.[6] Thus, the development of therapeutic strategies for treating ALI is crucial.

Ferroptosis, a special kind of programmed cell death, is characterized by the accumulation of iron and membrane lipid peroxidation products during the cell death.[7] Ferrostatin-1 is an inhibitor of ferroptosis that can reverse lipopolysaccharide (LPS)-induced increase of malondialdehyde (MDA) and total iron levels.[8] Moreover, ferroptosis modulates Nrf2/ARE signaling pathway and participates in LPS-induced ALI.[9] Furthermore, ferroptosis has been demonstrated to be involved in intestinal ischemia or reperfusion (I/R) injury in ALI.[10] IASPP, an inhibitor of p53, inhibits ferroptosis in intestinal I/R-induced ALI through regulation of Nrf2/HIF-1α/TF signaling pathway.[11] Thus, these findings indicate that ferroptosis may serve as a potential target for ALI treatment.

Src homology 2 (SH2)-containing protein tyrosine phosphatase 2 (SHP2) is a kind of protein tyrosine phosphatase expressed in the lung tissues.[12] SHP2 is highly expressed in lungs of smoking mice, and can be a potential target for treating inflammation in cigarette smoke (CS)-induced pulmonary diseases.[13] Besides, the knockdown of SHP2 retains epithelial barrier dysfunction, which is of great benefit to lung inflammation.[12] However, the role of SHP2 in LPS-induced ALI remains unclear.

In this study, we found that SHP2 was highly expressed in LPS-induced ALI mouse modes. More importantly, knockdown of SHP2 significantly attenuated LPS-induced lung injury and suppressed ferroptosis. To investigate the role and mechanism of SHP2 in LPS-induced ALI, loss-of-function experiments were performed in LPS-induced ALI mouse model *in vivo* and LPS-induced MLE-12 cell model *in vitro*. Understanding the role of SHP2 in ferroptosis may help promote the development of therapies for ALI.

Materials and Methods

All animal experiments in this study were performed in accordance with the Guide for the Care and Use of Laboratory Animals and were approved by Linfen People's Hospital.

Animal models

In this study, a total of 36 male C57BL/6 mice (8–10 weeks old) were randomly divided into six groups (n = 6 per group): Sham, LPS, sham + AAV-shNC, sham + AAV-shSHP2, LPS + AAV-shNC, and LPS + AAV-shSHP2. To induce ALI mouse model, the mice received intratracheal instillation with 50 μL of LPS solution (0.2 g/L) plus 0.9% NaCl (LPS group), while those mice that received intratracheal instillation with 0.9% NaCl (Sham group) were used as the control. The AAV-shSHP2 and corresponding control AAV-shNC were purchased from Hanbio (China). Twenty-one days before LPS treatment, the mice were anesthetized by sodium pentobarbital and given 4×10^{10} vector genomes (vg) of AAV-shNC or AAV-shSHP2 (6×10^{12} vg/mL) dissolved in 50 μL phosphate buffered saline (PBS) via intratracheal instillation to reduce SHP2 expression. All the mice were sacrificed at 24 h post LPS stimulation. To collect the bronchoalveolar lavage fluid (BALF), the right lung of the mouse was ligated, and the left lung was lavaged. Finally, the lung tissues were removed for further experiments.

Lung wet-to-dry weight (W/D) ratio

After weighing the fresh lung tissue, these were placed in the oven for 48 h. After this, the lung tissue was weighed again, and the lung W/D ratio was calculated.

Histopathological lung examination

The lung tissues were embedded in paraffin, cut into 4 μm sections, dewaxed, rehydrated, and then stained with hematoxylin and eosin (H&E) solution (ab245880, Abcam, UK) to estimate pathological changes and lung injury score. The stained sections were observed under a light microscope. The lung injury score was evaluated by the degree of lung injury, based on hyaline membranes, neutrophils infiltration, alveolar septal thickening, and proteinaceous debris.[14]

Immunofluorescence (IF) assay

Lung tissue sections were deparaffinized and permeabilized before incubation with anti-SHP2 antibody (ab32083; 1:400; Abcam, UK) overnight at 4°C. The sections were then washed with PBS and incubated with goat anti-rabbit IgG Alexa Fluor®488 (ab150077; 1:1000; Abcam, UK) and visualized under a fluorescence microscope (Leica, Germany).[15,16]

Bronchoalveolar lavage fluid analysis

The total cells in the BALF were counted with a hemocytometer.

The protein concentration in the BALF was measured with the BCA Protein Assay kit (23227; Thermo Fisher Scientific, USA).

Lung capillary leakage assay

The Evans blue dye (E2129, Sigma-Aldrich, USA) was used to assess lung capillary leakage, which is used to measure

the increase in pulmonary microvascular leak. The mice received intravenous injection of Evans blue dye (20 mg/kg). Once the mice were sacrificed, the right lung was homogenized with formamide and placed at 37°C for 18 h. After being quantified at optical density (OD) 620 nm, the Evans blue value was calculated as micrograms of Evans blue dye per gram of lung tissues.

Cell culture and treatment

The mouse lung epithelial cell line MLE-12 was obtained from ATCC (USA), cultured in DMEM (12491023; GIBCO, USA) medium containing 10% fetal bovine serum (12664025; FBS, Gibco, USA) in 5% CO_2 at 37°C.

For transfection, the MLE-12 cells were transfected with shNC or shSHP2 (Hanbio, China) with lipofectamine 2000 (11668027; Invitrogen, USA). For cotransfection, the MLE-12 cells were cotransfected with shNC or shSHP2 and pcDNA3-NC or pcDNA3-ACSL4 using lipofectamine 2000. For LPS treatment, the MLE-12 cells after transfection were treated with 100 μg/mL LPS for 24 h.

Cell viability assay

The cell viability was measured by Cell Counting Kit-8 (CCK-8) (C0037; Beyotime, China). The cells after treatment were seeded in 96-well plates at a density of 2×10^4/well. Thereafter, the cells were washed with PBS, added with CCK-8 solution, and incubated at 37°C for 2 h. The absorbance of these cells at 450 nm was measured using a microplate reader (BioTek, USA).

Evaluation of malondialdehyde (MDA), LDH, GSH, and iron levels

The MDA, LDH, GSH, and iron concentrations in tissues and cell lysates were assessed by the following kits: mouse malondialdehyde (MDA) (A003-1-2; Njjcbio, China), mouse lactate dehydrogenase (LDH) (A020-2-2; Njjcbio, China), mouse glutathione (GSH) (A006-2-1; Njjcbio, China), and iron assay kit (A039-1-1; Njjcbio., China), respectively.

Reactive Oxygen Species (ROS) assay

Reactive oxygen species levels of cells were detected with a fluorescent probe, 2',7'-dichlorodihydrofluorescein (DCHF) (4091990; MedChemExpress, USA). The cells were stained with 25 μM DCHF, and the fluorescence was monitored under a fluorescence microscope (Leica).

Quantitative real time-PCR (qRT-PCR) assay

Total-RNA from cells or tissues was isolated using RNAiso Plus (9109; TaKaRa, Japan). The cDNA was then synthesized with cDNA Reverse Transcription kit (RR037a; TaKaRa, Japan). Subsequently, the qRT-PCR was performed with SYBR Premix Ex Taq™ (DRR041A; TaKaRa, Japan).

Western blot

The protein in cells and tissues were isolated using a lysis buffer and then loaded onto the polyacrylamide gel. The blot was incubated with SHP2 antibody (ab32083; 1:400; Abcam, UK), ACSL4 antibody (ab155282; 1:400; Abcam, UK), GPX4 antibody (ab125066; 1:400; Abcam, UK), SLC7A11 antibody (ab307601; 1:400; Abcam, UK), or ß-actin antibody (1:400; Abcam, UK) overnight at 4°C after gel running, transferring, and blocking.[17] The blots were then incubated with horseradish peroxidase (HRP)-conjugated secondary antibody (ab6721, ab6728; 1:5000; Abcam, UK), followed by visualization with ECL (P0018M; Beyotime, China).[18]

Statistical analysis

All the data from normal distributions in the current study were expressed as mean ± standard deviation (SD) and analyzed with the GraphPad Prism 7.0 software (GraphPad Software, USA). The variance homogeneity of data was assessed using Levene's test. The comparisons between the two groups were analyzed by unpaired student's *t*-test. P-value less than 0.05 was considered statistically significant.

Results

SHP2 was upregulated in LPS-induced ALI models in vivo and in vitro

To confirm the successful establishment of LPS-induced ALI model, pathological changes in lung tissues were detected by H&E staining. As shown in Figure 1, the lung tissues in mice suffered with LPS administration displayed destroyed pulmonary architecture, notable inflammatory cell infiltration, alveolar edema, and thickened alveolar septa compared to Sham mice. Moreover, the lung injury score in LPS-induced mice was significantly higher than that in Sham mice (Figure 1B). Compared to the Sham mice, both mRNA and protein levels of SHP2 were remarkably promoted in LPS-induced mice (Figures 1C and 1D). Besides, the IF assay further confirmed that SHP2 was distributed in LPS-induced mice, which was rarely expressed in Sham mice (Figure 1E). Consistently, through establishment of the LPS-induced ALI model *in vitro*, both mRNA and protein levels of SHP2 were enhanced in LPS-induced MLE-12 cells (Figures 1F and 1G). These findings revealed that SHP2 was upregulated in LPS-induced ALI mice and MLE-12 cells.

Knockdown of SHP2 attenuated LPS-induced lung injury

To verify the function of SHP2 in LPS-induced ALI, the mice received AAV-shNC or AAV-shSHP2 administration. At first, LPS-induced expression of SHP2 was decreased by AAV-shSHP2 (Figure 2A). Moreover, knockdown of SHP2 significantly attenuated LPS-induced pulmonary architecture, notable inflammatory cell infiltration, alveolar edema, and thickened alveolar septa (Figure 2B).

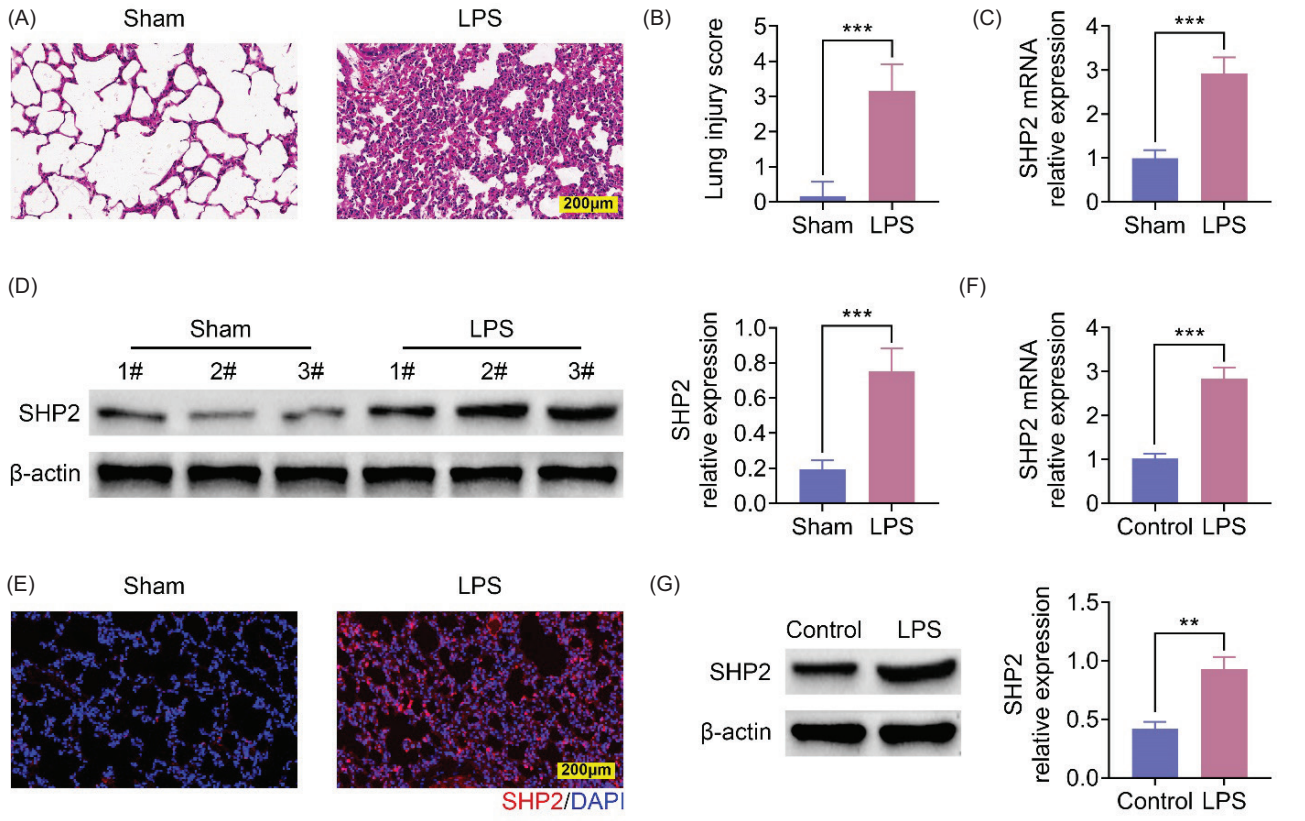

Figure 1 SHP2 was upregulated in LPS-induced ALI models *in vivo* and *in vitro*. The LPS-induced ALI mouse model was successfully established. (A, B) The pathological changes of lung tissues in Sham and LPS-induced mice were examined by H&E staining, and the lung injury score was evaluated. (C, D) Both mRNA and protein levels of SHP2 in lung tissues were upregulated in LPS-induced mice. (E) The distribution of SHP2 in lung tissues was determined by IF staining. (F, G) The MLE-12 cells were pretreated with or without LPS. Consistently, the mRNA and protein levels were enhanced in LPS-induced MLE-12 cells. Each experiment was repeated thrice. **P < 0.01, ***P < 0.001.

Consistently, the lung injury score was declined after AAV-shSHP2 administration in LPS-induced mice (Figure 2C). It has been reported that sepsis severely damages the microvessles of the lungs and increases the protein concentration in the BALF.[19] To evaluate the permeability of pulmonary microvasculature, the protein concentration in BALF was detected. As shown in Figure 2D, LPS damaged the lung microvessles, while sh-SHP2 mitigated LPS-induced disruption of pulmonary microvessles. The inflammatory response can be evaluated by counting the total number of inflammatory cells. The results (Figure 2E) suggested that LPS administration increased the number of the cells in BALF, which was greatly reduced by knockdown of sh-SHP2. Moreover, the lung W/D ratio was increased in LPS-induced mice compared to that in Sham group. Nevertheless, the treatment with AAV-shSHP2 could ameliorate LPS-induced pulmonary edema (Figure 2F). As shown in Figure 2G, LPS dramatically increased Evans blue accumulation in the lungs, which was reduced by the knockdown of SHP2, suggesting that knockdown of SHP2 reduced LPS-induced increase of lung vascular permeability. Thus, these findings demonstrated that knockdown of SHP2 attenuated LPS-induced lung injury, microvessles damage, pulmonary edema, and the increase in lung vascular permeability.

Knockdown of SHP2 attenuated LPS-induced MLE-12 cell ferroptosis

In order to explore the effect of SHP2 on LPS-treated MLE-12 cells, shSHP2 or shNC was transfected into MLE-12 cell with or without LPS treatment. LPS enhanced SHP2 expression in MLE-12 cells, which was decreased by shSHP2 administration (Figure 3A). More importantly, LPS decreased MLE-12 cellular viability, which was partly increased by shSHP2 (Figure 3B). LPS promoted LDH activity, MDA, and iron levels, and suppressed GSH expression in MLE-12 cells, which were reversed by knockdown of SHP2 (Figures 3C-3E). Interestingly, the expression of ferroptosis-related biomarkers including GPX4 and SLC7A11 was reduced by LPS treatment, which was reversed by shSHP2 (Figure 3F). These findings revealed that knockdown of SHP2 attenuated LPS-induced MLE-12 cell ferroptosis.

Knockdown of SHP2 attenuated LPS-induced ferroptosis in lung tissues

To confirm the role of SHP2 in LPS-induced ferroptosis *in vivo*, the LDH activity, MDA, iron, and GSH levels were measured. Consistent with the *in vitro* results, LPS

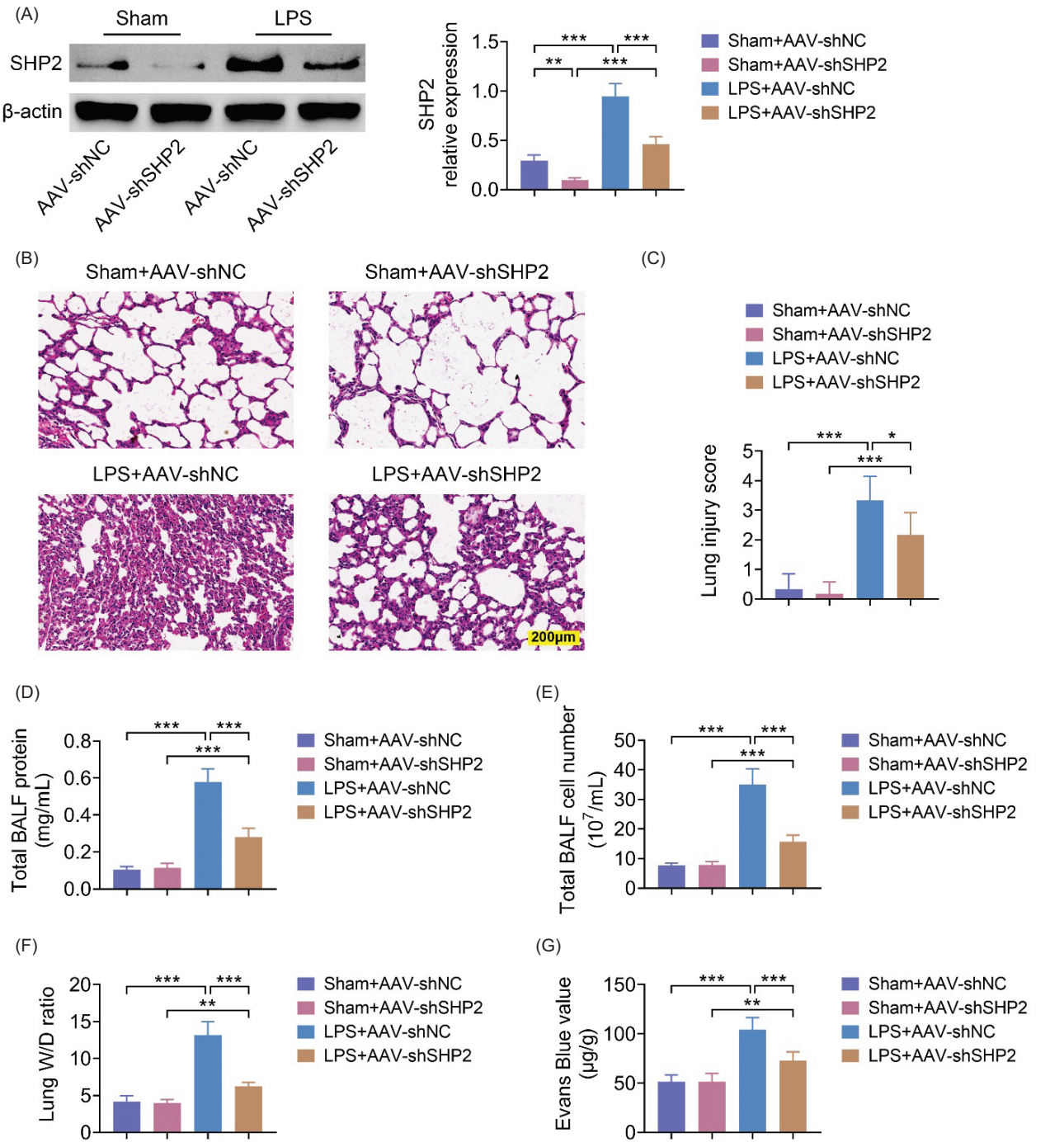

Figure 2 Knockdown of SHP2 attenuated LPS-induced ALI. The Sham and LPS group received AAV-shNC or AAV-shSHP2 administration. (A) The expression of SHP2 was detected by western blot. (B, C) The pathological changes were assessed by H&E staining, and the lung injury score was evaluated. (D) The damages the microvessles of the lung were determined by the measurement of protein concentration in the BALF. (E) The number of the cells in BALF was used to assess the inflammatory response. (F) The LPS-induced pulmonary edema was alleviated by AAV-shSHP2. (G) AAV-shSHP2 reduced the LPS-induced increase of Evans blue value in lung tissues. Each experiment was repeated thrice. *P < 0.05, **P < 0.01, ***P < 0.001.

promoted LDH activity, MDA, and iron levels in lung tissues, but reduced the GSH level. Nevertheless, these changes were abolished by knockdown of SHP2 (Figures 4A-C). Moreover, LPS induced the accumulation of ROS in lung tissues, which was rescued by shSHP2 (Figure 4D). As expected, LPS suppressed GPX4 and SLC7A11 expression in lung tissues, while AAV-shSHP2 dramatically enhanced their expression (Figure 4E). Therefore, these results indicated that knockdown of SHP2 attenuated LPS-induced ferroptosis in lung tissues.

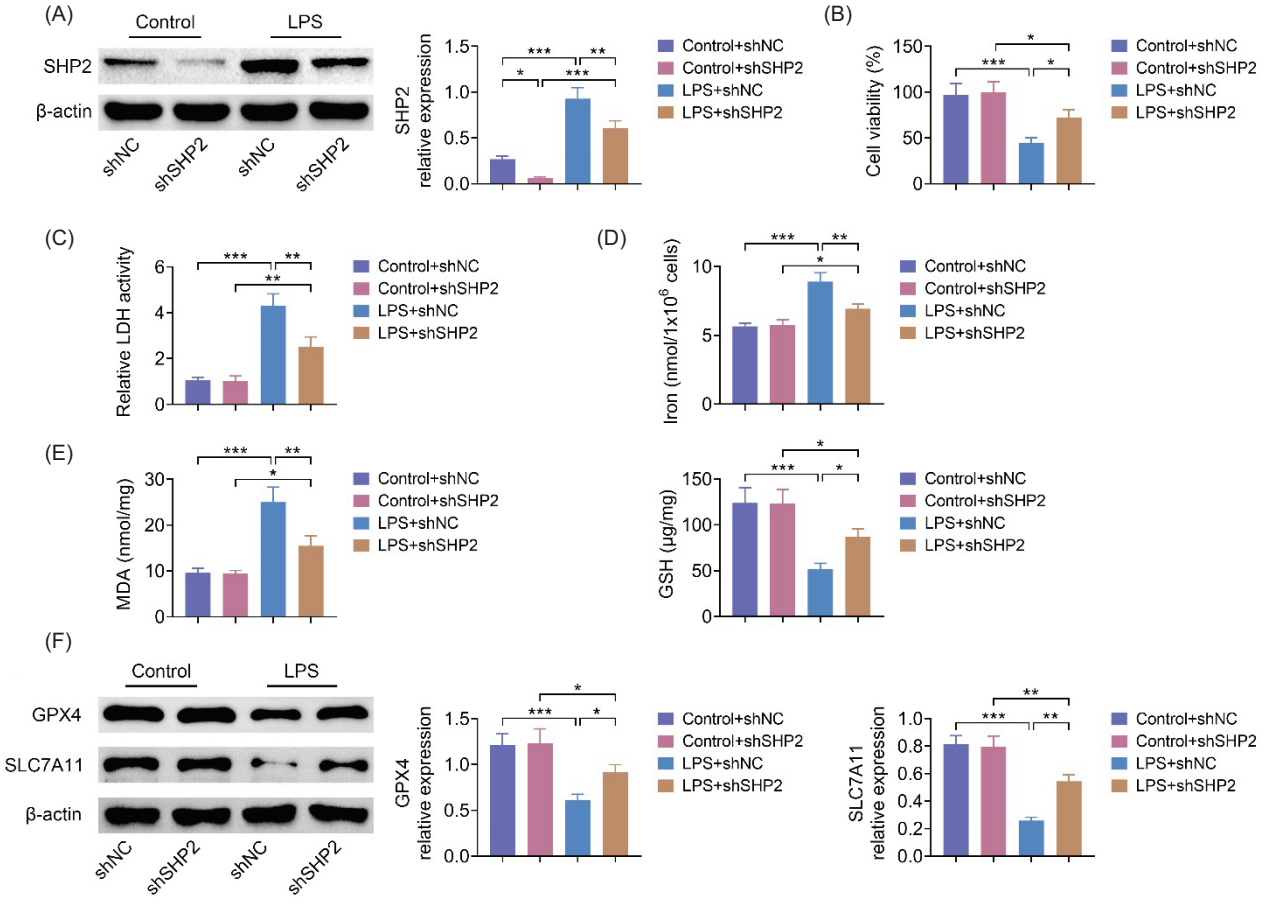

Figure 3 Knockdown of SHP2 attenuated LPS-induced MLE-12 cell ferroptosis. The shNC or shSHP2 was transfected into MLE-12 cells with or without LPS treatment. (A) The SHP2 expression was detected by western blot. (B) The cell viability was evaluated by CCK-8 assay. The LDH (C), iron and GSH (D), MDA (E) levels were measured by commercial kits. (F) The expression of ferroptosis-related biomarkers including GPX4 and SLC7A11 were determined by western blot. Each experiment was repeated thrice. *P < 0.05, **P < 0.01, ***P < 0.001.

SHP2 could modulate ACSL4 expression

It has been reported that SHP2 regulated the expression of ACSL4.[20] Interestingly, LPS enhanced both ACSL4 mRNA and protein levels in lung tissues, while these changes were reversed by AAV-shSHP4 (Figures 5A and 5B). Similarly, both ACSL4 mRNA and protein levels were enhanced in LPS-induced MLE-12 cells compared to control cells, which were abolished by knockdown of SHP2 (Figures 5C and 5D). These findings suggested that SHP2 could modulate ACSL4 expression.

Knockdown of SHP2 attenuated LPS-induced ferroptosis via downregulating ACSL4 expression in MLE-12 cells

To further investigate the effect of SHP2 on ferroptosis through regulating ACSL4 expression, overexpression of ACSL4 was applied in our study. As the results (Figure 6A) suggested, ACSL4 was successfully overexpressed in MLE-12 cells. Interestingly, the cell viability in the LPS + shSHP2 + ACSL4 group was lower than that in the LPS + shSHP2 + NC group, indicating the rescue effect of ACSL4 on LPS + shSHP2 cell death (Figure 6B). Moreover, overexpression of ACSL4 promoted the shSHP2-induced reduction of LDH, iron, and MDA levels, whereas it reduced the shSHP2-induced promotion of GSH level (Figures 6C-6E). Besides, shSHP2-induced increases in GPX4 and SLC7A11 expression were notably decreased by overexpressed ACSL4 (Figure 6F). These results suggested that knockdown of SHP2 attenuated LPS-induced ferroptosis via downregulation of expression of ACSL4 in MLE-12 cells.

Discussion

In this study, we demonstrated that SHP2 was upregulated in LPS-induced ALI mice and LPS-induced MLE-12 cells. In loss-of function experiment, knockdown of SHP2 attenuated LPS-induced lung injury, microvessles damage, pulmonary edema, and the increase of lung vascular permeability *in vivo*. Mechanically, shSHP2 rescued LPS-induced increases in LDH activity, MDA, and iron levels, and a decrease in GSH level, as well as the accumulation of ROS *in vivo* and *in vitro*, leading to an alleviation of LPS-induced ferroptosis.

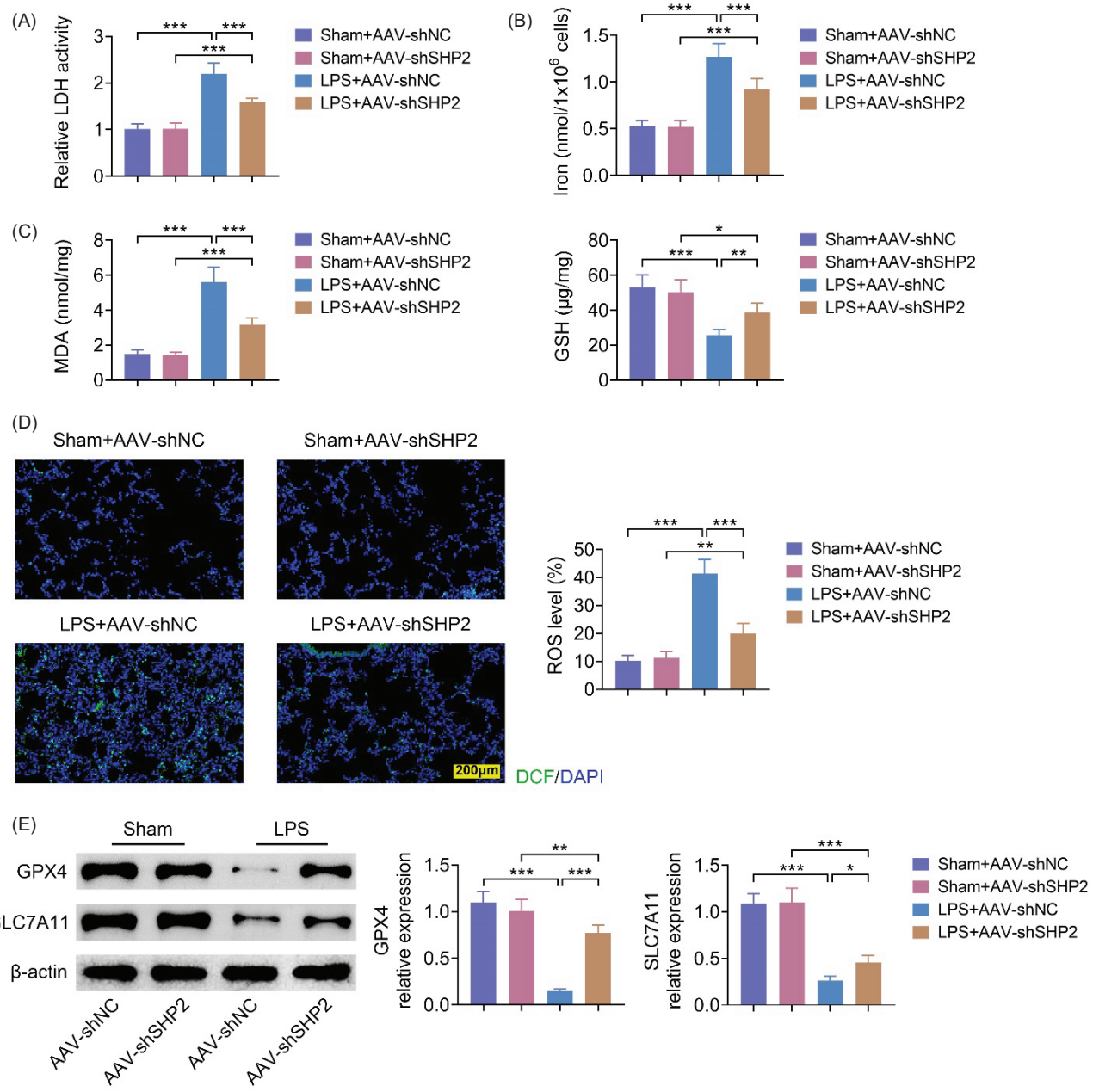

Figure 4 Knockdown of SHP2 attenuated LPS-induced ferroptosis in lung tissues. The LDH activity (A), GSH and iron (B), MDA (C) levels in lung tissues were measured by commercial kit. (D) The accumulation of ROS in lung tissues was measured by DCFH-DA staining assay. (E) The expression of GPX4 and SLC7A11 expression were determined by western blot. Each experiment was repeated thrice. *P < 0.05, **P < 0.01, ***P < 0.001.

Notably, shSHP2 reduced the expression of ACSL4. In the rescued experiments, overexpression of ACSL4 abolished the shSHP2-induced reductions of LDH activity, MDA, and iron levels, and a promotion of GSH level, thereby aggravating the LPS-induced ferroptosis. These findings revealed that knockdown of SHP2 attenuated LPS-induced ferroptosis via downregulating the ACSL4 expression in ALI, providing a novel sight for ALI treatment.

ALI can be caused by various pulmonary factors (such as pulmonary inflammation) and extrapulmonary factors (such as sepsis and surgery), with pathological manifestations including injury of pulmonary capillary, diffuse alveolar and interstitial edema.[21,22] In this study, LPS administration led to destroyed pulmonary architecture, notable inflammatory cell infiltration, alveolar edema, and thickened alveolar septa, indicating the successful establishment of LPS-induced ALI mouse model. However, the occurrence of ALI might be involved in the cell death, oxidative stress, excessive accumulation of ROS, and uncontrolled inflammatory response.[23] Normally, the lung maintains iron homeostasis depending on the phagocytosis of macrophages, antioxidant molecules, and transferrin in secretion.[24] Oxidative stress-induced damage in the lungs is activated when the protective mechanism is disrupted

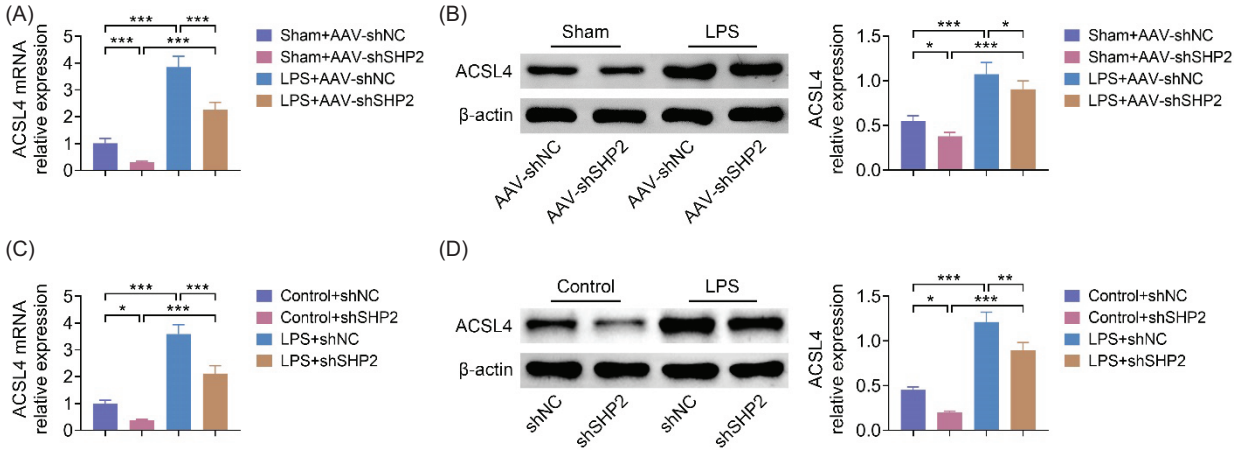

Figure 5 SHP2 could modulate ACSL4 expression. (A, B) The ACSL4 mRNA and protein levels in lung tissues were evaluated by qRT-PCR and western blot. (B) The ACSL4 mRNA and protein levels in MLE-12 cells were evaluated by qRT-PCR and western blot. Each experiment was repeated thrice. *P < 0.05, **P < 0.01, ***P < 0.001.

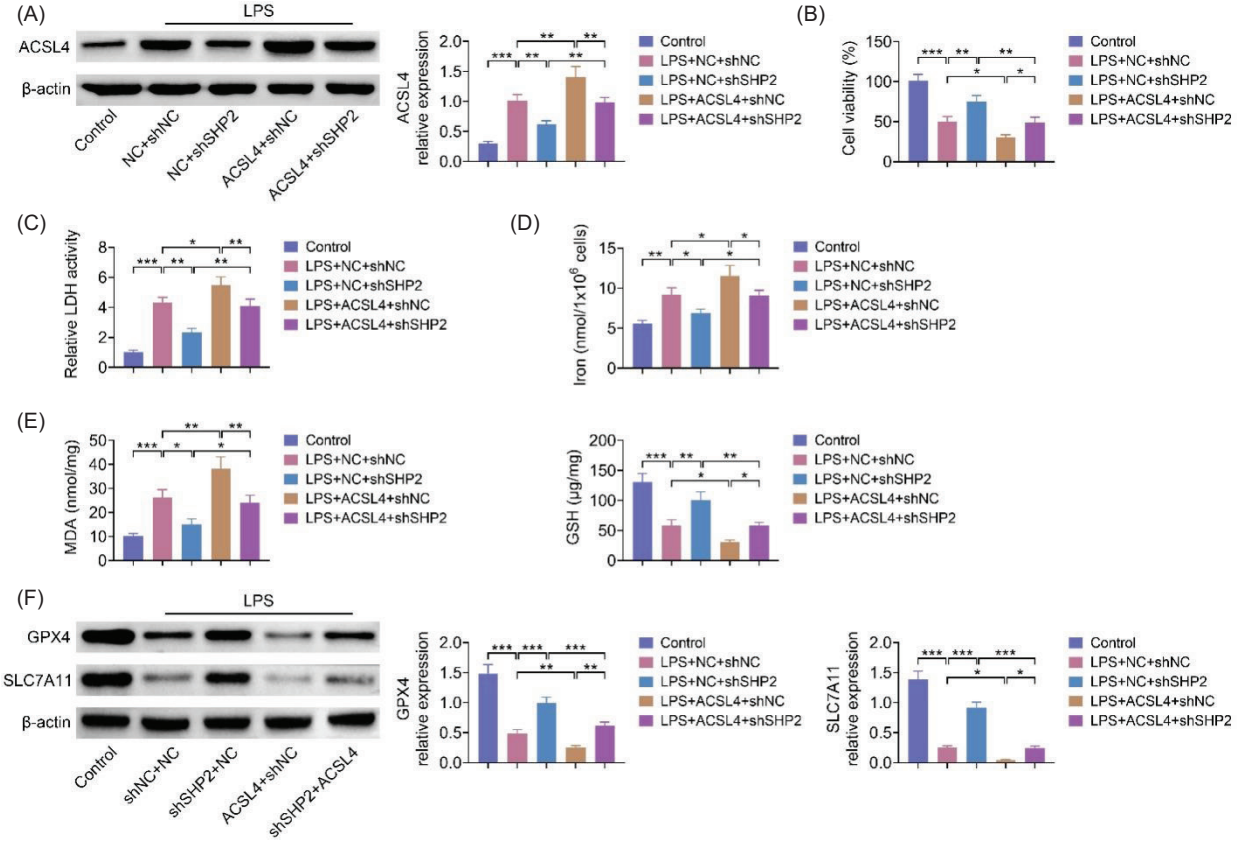

Figure 6 Knockdown of SHP2 attenuated LPS-induced ferroptosis via downregulating ACSL4 expression in MLE-12 cells. The MLE-12 cells with LPS treatment were cotransfected with shNC or shSHP2 and NC or ACSL4. (A) The expression of ACSL4 was detected by western blot. (B) The cell viability was determined by CCK-8 assay. The LDH activity (C), GSH and iron (D), MDA (E) levels in MLE-12 cells were measured by commercial kit. (F) The expression of GPX4 and SLC7A11 expression in MEL-12 cells were assessed by western blot. Each experiment was repeated thrice. *P < 0.05, **P < 0.01, ***P < 0.001.

by endogenous or exogenous factors.[25] Interestingly, excess iron and decrease of total GSH have been found in ALI patients.[26] Iron accumulation activates inflammatory response and oxidative stress, eventually leading to lung damage through ferroptosis.[27] In this study, we found that LPS administration significantly enhanced ferroptosis in lung tissues and MLE-12 cells, which was in line with previous studies.

Ferroptosis, an iron-dependent programmed cell death, is regulated by lipid oxidation, and is implicated in many disease pathologies.[28] Increasing evidence have shown that ferroptosis plays an essential role in pathogenesis of ALI. Li et al. have demonstrated that panaxydol attenuated ferroptosis against LPS-induced ALI.[29] In a recent study, JMJD3 deficiency alleviated LPS-induced ALI by inhibiting alveolar epithelial ferroptosis.[30] Sevoflurane inhibited ferroptosis and exerted protective role against LPS-induced ALI.[31] These findings indicated that the interruption of ferroptosis may be a novel therapeutic strategy for ALI. SHP2 modulated various pathological and physiological processes via modulating inflammation and fibroblasts.[32] SHP2 deficiency regulated activation of macrophage and prevented radiation-induced lung injury.[33] Knockout of *SHP2* in lung epithelia reduced pulmonary inflammation in mice.[13] However, the association between SHP2 and ferroptosis remains unclear. The expression of ferroptosis markers, including GPX4 and SLC7A11, are downregulated, while MDA level and total iron are significantly increased after LPS intervention.[8] Consistently, our results proved that knockdown of SHP2 promoted GPX4 and SLC7A11 expression, reduced MDA and total iron levels after LPS administration, revealing that knockdown of SHP2 attenuated LPS-induced ALI via suppression of ferroptosis. This might be the first time that the suppressive effect of shSHP2 on ferroptosis is being verified. However, the mechanism of shSHP2 in ferroptosis is still unknown.

The activation of SHP2 relies on cAMP-dependent pathway and then modulates ACSL4 expression. Notably, knockdown of SHP2 reduced both mRNA and protein levels of ACSL4, which was observed in this study.[20] Mechanically, ACSL4, a vital enzyme in proferroptotic lipid metabolism, is required for forming phospholipid hydroperoxide.[34] Knockdown of ACSL4 partially abrogates the enhanced lipid ROS and cell death in lung injury, indicating that lack of ACSL4 exerts a less susceptibility to ferroptosis.[35] In this study, we confirmed that knockdown of SHP2 reduced the ACSL4 expression, subsequently decreased the accumulation of ROS and the susceptibility to ferroptosis, thereby leading to the alleviation of ferroptosis and LPS-induced ALI. Our study also had several limitations. The mechanism of regulation of SHP2 on ACSL4 remained undisclosed, and clinical samples were not involved in to support our findings. Further studies are needed to verify the modulation of SHP2 on ACSL4 expression in ALI.

In summary, our findings demonstrated that knockdown of SHP2 attenuated LPS-induced ferroptosis via downregulation of ACSL4 expression, which might provide a novel sight for ALI treatment.

Acknowledgments

Not applicable.

Funding

This work was supported by the Natural Science Foundation of the Linfen People's Hospital (Grant No. T20220609032).

Availability of Data and Materials

All data generated or analyzed during this study are included in this published article.

The datasets used and/or analyzed during this study are available from the corresponding author upon request.

Competing Interests

The authors state that there are no conflicts of interest to disclose.

Ethics Approval

Ethical approval was obtained from the Ethics Committee of Linfen People's Hospital.

Authors' Contribution

All authors contributed to the study conception and design. Material preparation and the experiments were performed by Bin Li. Data collection and analysis were performed by Zhan Wang, Jiayang Yuan, Dachuan Liang, and Yanrong Cheng. The first draft of the manuscript was written by Zheng Wang, and all authors commented on previous versions of the manuscript. All authors read and approved the final manuscript.

References

1. Ashbaugh DG, Bigelow DB, Petty TL, Levine BE. Acute respiratory distress in adults. Lancet. 1967;2(7511):319–23. https://doi.org/10.1016/s0140-6736(67)90168-7
2. Xu B, Chen SS, Liu MZ, Gan CX, Li JQ, Guo GH. Stem cell derived exosomes-based therapy for acute lung injury and acute respiratory distress syndrome: A novel therapeutic strategy. Life Sci. 2020;254:117766. https://doi.org/10.1016/j.lfs.2020.117766
3. Kaku S, Nguyen CD, Htet NN, Tutera D, Barr J, Paintal HS, et al. Acute respiratory distress syndrome: Etiology, pathogenesis, and summary on management. J Intensive Care Med. 2020;35(8):723–37. https://doi.org/10.1177/0885066619855021
4. Matthay MA, Zemans RL, Zimmerman GA, Arabi YM, Beitler JR, Mercat A, et al. Acute respiratory distress syndrome. Nat Rev Dis Primers. 2019;5(1):18. https://doi.org/10.1038/s41572-019-0069-0

5. Wang M, Cai Q. Phillygenin attenuates LPS-induced acute lung injury of newborn mice in infantile pneumonia. Signa Vitae. 2021;17(4):171–7.
6. Zoulikha M, Xiao Q, Boafo GF, Sallam MA, Chen Z, He W. Pulmonary delivery of siRNA against acute lung injury/acute respiratory distress syndrome. Acta Pharm Sin B. 2022;12(2):600–20. https://doi.org/10.1016/j.apsb.2021.08.009
7. Li J, Cao F, Yin HL, Huang ZJ, Lin ZT, Mao N, et al. Ferroptosis: Past, present and future. Cell Death Dis. 2020;11(2):88. https://doi.org/10.1038/s41419-020-2298-2
8. Liu P, Feng Y, Li H, Chen X, Wang G, Xu S, et al. Ferrostatin-1 alleviates lipopolysaccharide-induced acute lung injury via inhibiting ferroptosis. Cell Mol Biol Lett. 2020;25:10. https://doi.org/10.1186/s11658-020-00205-0
9. Yu JB, Shi J, Gong LR, Dong SA, Xu Y, Zhang Y, et al. Role of Nrf2/ARE pathway in protective effect of electroacupuncture against endotoxic shock-induced acute lung injury in rabbits. PLoS One. 2014;9(8):e104924. https://doi.org/10.1371/journal.pone.0104924
10. Dong H, Qiang Z, Chai D, Peng J, Xia Y, Hu R, et al. Nrf2 inhibits ferroptosis and protects against acute lung injury due to intestinal ischemia reperfusion via regulating SLC7A11 and HO-1. Aging (Albany NY). 2020;12(13):12943–59. https://doi.org/10.18632/aging.103378
11. Li Y, Cao Y, Xiao J, Shang J, Tan Q, Ping F, et al. Inhibitor of apoptosis-stimulating protein of p53 inhibits ferroptosis and alleviates intestinal ischemia/reperfusion-induced acute lung injury. Cell Death Differ. 2020;27(9):2635–50. https://doi.org/10.1038/s41418-020-0528-x
12. Ouyang W, Liu C, Pan Y, Han Y, Yang L, Xia J, et al. SHP2 deficiency promotes *Staphylococcus aureus* pneumonia following influenza infection. Cell Prolif. 2020;53(1):e12721. https://doi.org/10.1111/cpr.12721
13. Li FF, Shen J, Shen HJ, Zhang X, Cao R, Zhang Y, et al. Shp2 plays an important role in acute cigarette smoke-mediated lung inflammation. J Immunol. 2012;189(6):3159–67. https://doi.org/10.4049/jimmunol.1200197
14. Wu X, Kong Q, Zhan L, Qiu Z, Huang Q, Song X. TIPE2 ameliorates lipopolysaccharide-induced apoptosis and inflammation in acute lung injury. Inflamm Res. 2019;68(11):981–92. https://doi.org/10.1007/s00011-019-01280-6
15. Bostani M, Rahmati M, Mard SA. The effect of endurance training on levels of LINC complex proteins in skeletal muscle fibers of STZ-induced diabetic rats. Sci Rep. 2020;10(1):8738. https://doi.org/10.1038/s41598-020-65793-5
16. Rahmati M, Rashno A. Automated image segmentation method to analyse skeletal muscle cross section in exercise-induced regenerating myofibers. Sci Rep. 2021;11(1):21327. https://doi.org/10.1038/s41598-021-00886-3
17. Rahmati M, Taherabadi SJ. The effects of exercise training on Kinesin and GAP-43 expression in skeletal muscle fibers of STZ-induced diabetic rats. Sci Rep. 2021;11(1):9535. https://doi.org/10.1038/s41598-021-89106-6
18. Rahmati M, Shariatzadeh Joneydi M, Koyanagi A, Yang G, Ji B, Won Lee S, et al. Resistance training restores skeletal muscle atrophy and satellite cell content in an animal model of Alzheimer's disease. Sci Rep. 2023;13(1):2535. https://doi.org/10.1038/s41598-023-29406-1
19. Hawiger J. Heartfelt sepsis: Microvascular injury due to genomic storm. Kardiol Pol. 2018;76(8):1203–16. https://doi.org/10.5603/KP.a2018.0146
20. Cooke M, Orlando U, Maloberti P, Podesta EJ, Cornejo Maciel F. Tyrosine phosphatase SHP2 regulates the expression of acyl-CoA synthetase ACSL4. J Lipid Res. 2011;52(11):1936–48. https://doi.org/10.1194/jlr.M015552
21. Li Y, Lin B. Icariside II regulates TLR4/NF-κB signaling pathway to improve septic lung injury. Signa Vitae. 2021;17(6):136–42.
22. Liu Y, Zhou S, Xiang D, Ju L, Shen D, Wang X, et al. Friend or foe? The roles of antioxidants in acute lung injury. Antioxidants (Basel). 2021;10(12):1956. https://doi.org/10.3390/antiox10121956
23. Xie W, Lu Q, Wang K, Lu J, Gu X, Zhu D, et al. miR-34b-5p inhibition attenuates lung inflammation and apoptosis in an LPS-induced acute lung injury mouse model by targeting progranulin. J Cell Physiol. 2018;233(9):6615–31. https://doi.org/10.1002/jcp.26274
24. Yin X, Zhu G, Wang Q, Fu YD, Wang J, Xu B. Ferroptosis, a new insight into acute injury. Front Pharmacol. 2021;12:709538. https://doi.org/10.3389/fphar.2021.709538
25. Liu X, Zhang J, Xie W. The role of ferroptosis in acute lung injury. Mol Cell Biochem. 2022;477(5):1453–61. https://doi.org/10.1007/s11010-021-04327
26. Ghio AJ, Carter JD, Richards JH, Richer LD, Grissom CK, Elstad MR. Iron and iron-related proteins in the lower respiratory tract of patients with acute respiratory distress syndrome. Crit Care Med. 2003;31(2):395–400. https://doi.org/10.1097/01.CCM.0000050284.35609.97
27. Yoshida M, Minagawa S, Araya J, Sakamoto T, Hara H, Tsubouchi K, et al. Involvement of cigarette smoke-induced epithelial cell ferroptosis in COPD pathogenesis. Nat Commun. 2019;10(1):3145. https://doi.org/10.1038/s41467-019-10991-7
28. Stockwell BR, Jiang X, Gu W. Emerging mechanisms and disease relevance of ferroptosis. Trends Cell Biol. 2020;30(6):478–90. https://doi.org/10.1016/j.tcb.2020.02.009
29. Yang D, Wang Y, Zheng Y, Dai F, Liu S, Yuan M, et al. Silencing of lncRNA UCA1 inhibited the pathological progression in PCOS mice through the regulation of PI3K/AKT signaling pathway. J Ovarian Res. 2021;14(1):48. https://doi.org/10.1186/s13048-021-00792-2
30. Peng J, Fan B, Bao C, Jing C. JMJD3 deficiency alleviates lipopolysaccharideinduced acute lung injury by inhibiting alveolar epithelial ferroptosis in a Nrf2-dependent manner. Mol Med Rep. 2021;24(5):807. https://doi.org/10.3892/mmr.2021.12447
31. Liu X, Wang L, Xing Q, Li K, Si J, Ma X, et al. Sevoflurane inhibits ferroptosis: A new mechanism to explain its protective role against lipopolysaccharide-induced acute lung injury. Life Sci. 2021;275:119391. https://doi.org/10.1016/j.lfs.2021.119391
32. Guo W, Xu Q. Phosphatase-independent functions of SHP2 and its regulation by small molecule compounds. J Pharmacol Sci. 2020;144(3):139–46. https://doi.org/10.1016/j.jphs.2020.06.002
33. Liu P, Li Y, Li M, Zhou H, Zhang H, Zhang Y, et al. Endothelial Shp2 deficiency controls alternative activation of macrophage preventing radiation-induced lung injury through notch signaling. iScience. 2022;25(3):103867. https://doi.org/10.1016/j.isci.2022.103867
34. Kagan VE, Mao G, Qu F, Angeli JP, Doll S, Croix CS, et al. Oxidized arachidonic and adrenic PEs navigate cells to ferroptosis. Nat Chem Biol. 2017;13(1):81–90.
35. Xu Y, Li X, Cheng Y, Yang M, Wang R. Inhibition of ACSL4 attenuates ferroptotic damage after pulmonary ischemia-reperfusion. FASEB J. 2020;34(12):16262–75. https://doi.org/10.1096/fj.202001758R